Mechanism of Photocurrent Generation from Bacteriorhodopsin on Gold Electrodes

Yoshitaka Saga and Tadashi Watanabe*

Institute of Industrial Science, University of Tokyo, Roppongi, Minato-ku, Tokyo 106-8558, Japan

Koichi Koyama and Tsutomu Miyasaka

Ashigara Research Laboratories, Fuji Photo Film Company, Ltd., Minami-ashigara, 250-0193, Japan

Received: May 6, 1998; In Final Form: November 3, 1998

Excitation of bacteriorhodopsin (bR) at an electrode−electrolyte interface generates transient photocurrents as evidenced by the turning of an incident light on and off. By use of a gold electrode as substrate, on which an oxide layer can be formed in a controlled manner, we have found two types of photocurrents, both originating in the excitation of bR. For the first type, arising most probably from the pH response of the surface oxide layer due to proton release/uptake by bR, the magnitude of photocurrent well paralleled the amount of surface oxide up to about one monolayer of Au_2O_3 and reached a maximum roughly equal to those observed on SnO_2 electrodes. The second type of photocurrent, being 3- to 4-fold smaller than the first one and essentially potential independent, arises presumably from simple charging, again through proton release/uptake by bR, of the electric double layer at the interface.

Introduction

Bacteriorhodopsin (bR), the sole protein in the purple membrane of *Halobacterium salinarium*, functions as a light-driven proton pump. The protein contains all-trans retinal as a chromophore bound to Lys-216 via a protonated Schiff base. Photoisomerization of the retinal from all-trans to 13-cis form triggers the transport of a proton from the cytoplasmic to the extracellular side, and the electrochemical potential thus built up across the membrane is then used for ATP synthesis.[1,2]

The proton transport in bR is a cyclic process. The reactions of retinal and protein during the photocycle, as confirmed by various spectroscopies, consists of interconversions of intermediate states denoted by J, K, L, M, N, and O.[3−6] In the transition from L to M, the proton on the Schiff base is transferred to Asp-85. A proton is subsequently released to the extracellular side, since the pK_a of the proton-releasing group in the extracellular domain is lowered by the protonation of Asp-85.[7−9] The decay of the M intermediate is accompanied by reprotonation of the Schiff base via Asp-96, and proton uptake by Asp-96 from the cytoplasmic side takes place in the transition from N to O.

Recently, photoelectric responses of bR at an electrode−electrolyte interface have been investigated,[10−16] where irradiation to bR-coated tin oxide (SnO_2) electrodes generated transient photocurrents by the turning on and off of the incident light. The origin of these photocurrents, however, has not been thoroughly understood yet.

Two groups proposed that the transient photocurrent is due to a pH change near the electrode.[14−16] Robertson and Lukashev examined the photocurrent responses of bR from the wild-type and a D96N mutant[14] where a nonprotonable asparagine replaced the protonable aspartate at position 96. The substitution of D96N made the rate of proton uptake much slower. The photocurrent from the D96N mutant by turning the light off was very weak in the amplitude and the decay was very slow, probably because of the low proton concentration change near the electrode resulting in the slowing of proton uptake rate.

Wang et al. observed photoelectric responses from bR on indium tin oxide (ITO) electrodes under both pulsed and continuous light excitations.[15,16] The polarity of the differential photocurrents by continuous illumination (denoted components D1 and D2) was reversed at low pH, and this phenomenon was rationalized by invoking the proton release/uptake sequence in the bR photocycle, based on an assumption that the photocurrent originates in the pH response of the oxide electrode[17,18] due to proton release and uptake by bR. It is of much interest to substantiate this interpretation.

On a gold electrode, exhibiting a relatively wide oxide-free potential range, oxides can be formed in a controlled fashion.[19] This has incited us to study, in the present work, the photoelectrochemical responses of bR on gold electrodes, to find the existence of two types of photocurrents, one of which being indeed the pH response of the surface oxide, Au_2O_3.

Materials and Methods

Purple membranes were prepared from cultured *Halobacterium salinarium* S9 according to the methods of Oesterhelt and Stoecknius[20] and were suspended in pure water until use.

A gold plate of 99.95% purity (Nilaco) was washed first with hot methanol then treated with hot concentrated nitric acid and rinsed thoroughly with distilled water. A 50-μL aliquot of the bR suspension, with an optical density of 10 at 1-cm path length at 570 nm, was deposited on a 1-cm^2 area of the electrode and then dried at room temperature and humidity to obtain a bR-immobilized electrode. Tin oxide (SnO_2) electrodes were also used for control experiments, according to the procedures described eleswhere.[10]

The photocurrent measurement setup was essentially the same as the one reported previously.[21] An Ushio Electric 500 W xenon

* To whom correspondence should be addressed: Institute of Industrial Science, University of Tokyo, Roppongi 7-22-1, Minato-ku, Tokyo 106-8558, Japan. Fax: +81-3-3401-5975. E-mail: watanabe@cc.iis.u-tokyo.ac.jp.

10.1021/jp982144u CCC: $18.00
Published on Web 12/12/1998

arc lamp Model UXL-500D-O served as the light source. Infrared radiation was removed with a 18-cm path length water cell, and a combination of Toshiba Glass cut filters O-56 and L-39 suppressed the short-wavelength light that tended to cause photocurrents due to excitation of the gold surface oxide itself.[19] For measurements of the photocurrent action spectra, the photon flux was determined by use of Koshin Kogaku interference filters (10-nm steps) and an Anritsu power meter Model MA9411.

A bR-immobilized electrode was mounted as a window (1 cm in diameter) of a photoelectrochemical cell. The supporting electrolyte was 0.1 M sodium sulfate in 10 mM phosphate buffer, pH = 7.2 (Iatron). The potential of the bR-immobilized electrode was controlled with a Toho Technical Research potentiostat Model 2000, with a Ag/AgCl and platinum wire as reference and counter electrodes, respectively. Photocurrents were measured with a Sony Tektronix oscilloscope Model TDS-340 after keeping the working electrode for 15 min at each potential. An NF Electric Instruments low-pass filter Model E-3201B was used in the measurements of photocurrent action spectra. Normally the measurements were repeated five times, and their averages are to be given below.

Each photocurrent measurement was followed by quantitation of surface oxide on the gold electrode from the area of an oxide reduction curve. A Hokuto Denko function generator Model HB-III was used to scan the potential at a rate of 10 mV s^{-1}, and current−potential curves were recorded on a Yokogawa X−Y recorder Model 3025. The electrode was held at an oxide-free potential (+0.1 V vs Ag/AgCl) before the photocurrent measurement at another potential.

Results

Photocurrent Patterns. Figure 1 depicts typical photocurrent response patterns from a bR-immobilized gold electrode held at +0.10, +0.75, and +0.90 V vs Ag/AgCl. At each potential, a cathodic transient current is observed by turning the light on, and an anodic transient current by turning the light off.[22] These patterns were essentially the same as those from bR-immobilized SnO_2 electrodes examined separately (Figure 6). However, the amplitude of the photocurrent from the bR-immobilized gold electrode at an oxide-free potential of +0.10 V is 3−4 times smaller than those from bR-immobilized SnO_2 electrodes.

A gold electrode undergoes surface oxidation substantially in a potential range positive of about +0.7 V vs Ag/AgCl. The photocurrents of Figure 1(b) and 1(c) are hence in such a potential range. The amplitude of the photocurrent at +0.90 V, Figure 1c, was a maximal one attained on gold electrodes, and was close to that generated from bR-immobilized SnO_2 electrodes (cf. Figure 6). For each trace in Figure 1, the action spectrum of the peak photoresponse was practically identical with the absorption spectrum of bR in suspension, as is seen in Figure 2. This indicates that the photocurrent results from excitation of bR on the electrode.

Photocurrent vs Surface Oxide. Under anodic polarization, a small stationary anodic photocurrent was observed even in the absence of bR. This is a photoelectrochemical response of gold oxide working as an n-type semiconductor electrode, as was reported in detail previously.[19]

On an anodic scan, surface oxidation of gold is seen to start on a small scale from around +0.5 V vs Ag/AgCl and substantially from +0.70 V, and pass through a maximum at +1.05 V. On the reverse scan, the oxide reduction curve peaks at around +0.50 V. In Figure 3 the oxide formation charge, obtained from integration of the reduction current−potential curve, is compared with the amplitude of the peak photocurrent as a function of electrode potential. Evidently there are two distinct branches in the photocurrent: the one growing in parallel with the progress of surface oxidation, but tending to level off at potentials beyond about +0.85 V, and the other (below +0.7 V) being independent of surface oxidation.

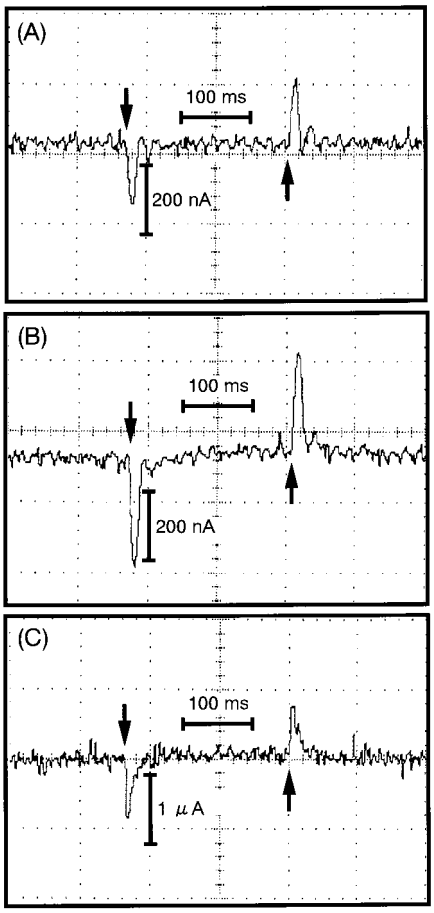

Figure 1. Photocurrent response patterns for bR on a gold electrode at three potentials. (A) +0.10, (B) +0.75, (C) +0.90 V vs Ag/AgCl. The arrows denote turning on and off of light. Light intensity, 40 mW cm^{-2}. Electrolyte, 0.1 M Na_2SO_4 in 10 mM phosphate buffer of pH 7.2.

For the potential range where surface oxidation was clearly noted on the reduction curve, the peak photocurrent is compared in Figure 4 with the oxide formation charge. The amplitude of the photocurrent well parallels the oxide formation charge up to around 300 μC cm^{-2} and levels off beyond this. The thickness of gold surface oxide can be estimated from the oxidation charge as follows. As a first approximation, the surface layer was assumed to be the main oxide, Au_2O_3,[19] for which the density has been evaluated to be 11 g cm^{-3}.[23] The roughness factor of the electrode surface is tentatively assumed to be 2 in view of literature values,[24−26] though its reliable determination is generally difficult.[26] By use of these values and the molar charge of $6F$, the monolayer of Au_2O_3 corresponds to a charge density of ca. 300 μC cm^{-2}. Therefore, Figure 4 demonstrates that the bR-derived photocurrent is roughly proportional to the amount of surface gold oxide up to a monolayer of the latter.

Higher Potential Range. Two factors could be envisaged as the cause for the photocurrent leveling off on gold electrodes at higher potentials. One is when a monolayer of Au_2O_3 is enough to exhibit the pH response of the oxide,[17,18] and the other factor is a potential-induced denaturation of bR. The latter possibility was examined by comparing the photocurrent at an

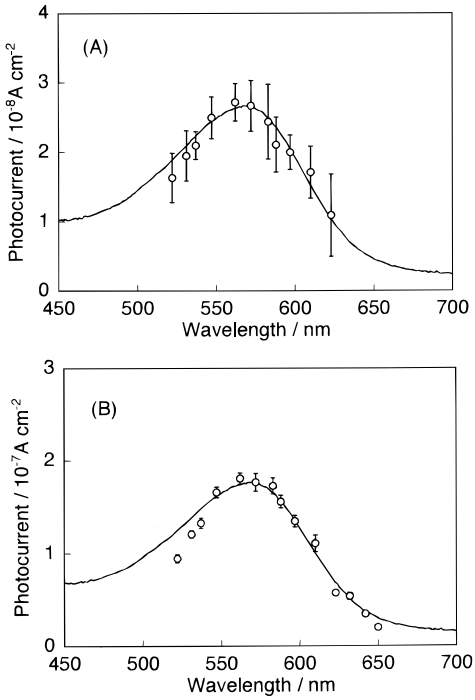

Figure 2. Action spectra of the peak photocurrent from bR on a gold electrode. (A) +0.10, (B) +0.80 V vs Ag/AgCl. Incident monochromatic photon flux, 1.19×10^{16} cm^{-2} s^{-1}. The solid curve represents the absorption spectrum of bR in suspension.

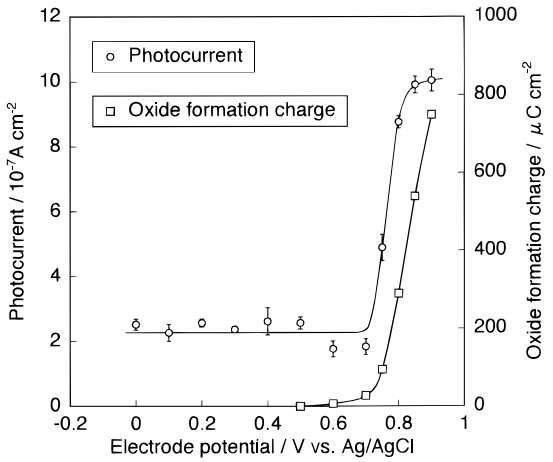

Figure 3. Dependencies of the photocurrent density from bR on a gold electrode and the oxide formation charge on the electrode potential.

oxide-free potential (+0.1 V) before and after a journey to higher potentials. The result is displayed in Figure 5 in the form of I/I_0 against the potential, where I_0 and I denote the photocurrent before and after the potential journey, respectively. As is seen, the photoactivity remains nearly constant at 1.0 ± 0.1, and hence the denaturation of bR is negligible up to a potential of +0.8 V, beyond which a denaturation appears to take place probably due to irreversible oxidation of bR.

Photocurrent from bR on SnO_2 Electrodes. Figure 6 depicts a typical photocurrent response from a bR-immobilized SnO_2 electrode at 0.0 V vs Ag/AgCl. The amplitude and kinetics are similar to those for a maximal photoresponse attained on gold electrodes (Figure 1 c). The peak photocurrents from a bR-immobilized SnO_2 electrode are plotted in Figure 7 against the electrode potential. The amplitude is almost independent of electrode potential from 0.0 V to +0.8 V, and the decrease in the photocurrent intensity at above +0.8 V is similar to that in Figure 5, probably due to the denaturation of bR.

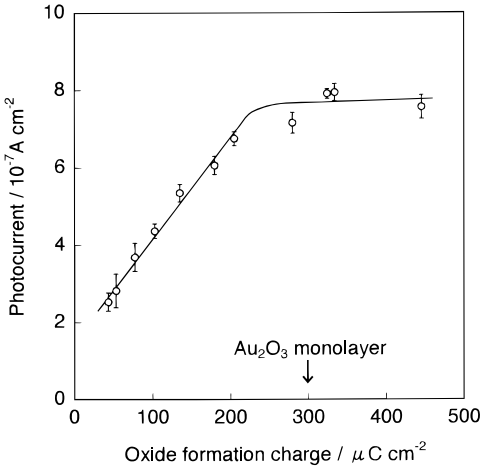

Figure 4. Photocurrent density as a function of the oxide formation charge on gold electrodes.

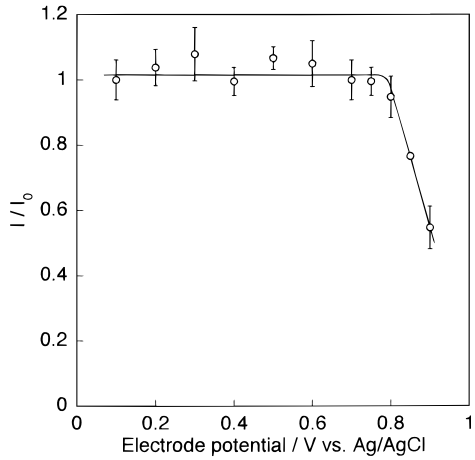

Figure 5. Ratio of the photocurrent density at +0.1 V after a potential journey to a positive potential on the abscissa (I) to that before the potential journey (I_0).

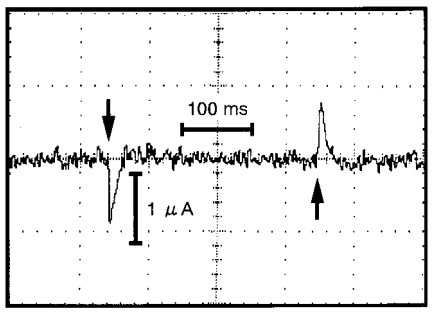

Figure 6. Photocurrent response patterns for bR on an SnO_2 electrode at 0.0 V vs Ag/AgCl. The arrows denote turning on and off of light.

Discussion

Excitation of bR on gold electrodes generates transient photocurrents by turning on and off of the incident light, in the same manner as on SnO_2 and ITO electrodes.[14−16] We were able to distinguish between two types of photocurrents on gold. One type commences to increase at around +0.7 V vs. Ag/AgCl, well in parallel with the start of surface oxidation, and is saturated beyond about +0.85 V. The saturation comes either from the sufficient thickness (more than a monolayer) or from some oxidative denaturation of bR at high potentials.

The mechanism of transient photocurrent generation from bR on a metal oxide electrode could be envisaged as shown in

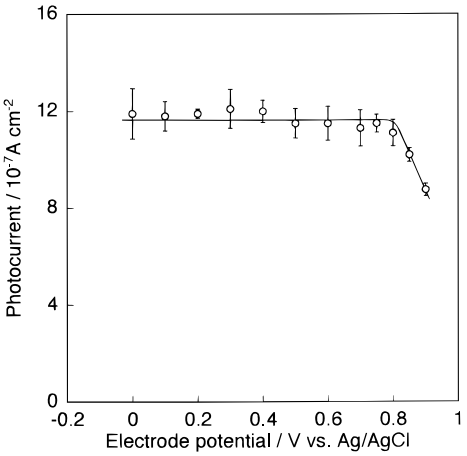

Figure 7. Potential dependence of the photocurrent density from bR on an SnO_2 electrode.

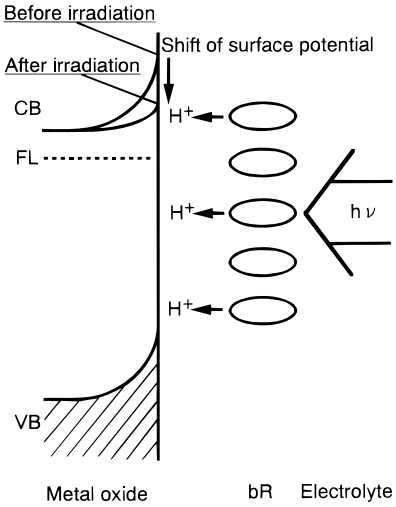

Figure 8. Mechanism of the transient photocurrent generation from bR on an oxide-covered metal electrode. CB, VB, and FL denote the conduction band, valence band, and Fermi level, respectively.

Figure 8, where the oxide is viewed as an n-type semiconductor electrode, as is the case for gold oxides.[19] On the surface of a semiconductor electrode in contact with an aqueous electrolyte, a proton dissociation equilibrium

$$\text{M-OH} \rightleftarrows \text{M}-\text{O}^- + \text{H}^+ \qquad (1)$$

is established for the surface hydroxide (M−OH). Protons released from excited bR in the interfacial region should shift the equilibrium to the left-hand side, and this shift is reflected in the anodic shift of the so-called flatband potential. In an ordinary situation where the semiconductor electrode is connected only to a reference electrode, the energy bands of the semiconductor are shifted anodically (downward in Figure 8), with no change in the band bending profile just beneath the surface. However, under potentiostatic conditions as in the present measurements, the potential shift can take place only on the surface, diminishing the band bending in the space charge layer. Such a change is equivalent, in terms of the potential profile in the space charge layer, to a cathodic polarization of the semiconductor electrode, giving rise to a transient capacitive (charging) current. The transient photocurrent at the onset of irradiation can be interpreted in this manner. Indeed, when a millivolt-level negative potential step was given to a bR-free gold electrode at a potential of +0.9 V vs Ag/AgCl in the dark,

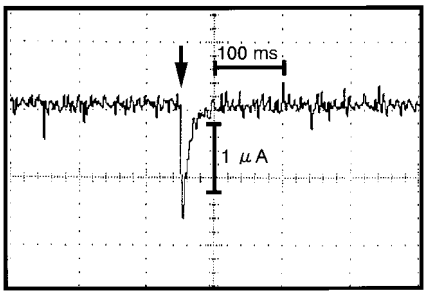

Figure 9. Transient current resulting from a −1 mV potential step applied to a gold electrode held at +0.9 V vs Ag/AgCl with no bR deposited. Electrolyte: 0.1 M Na_2SO_4 in 10 mM phosphate buffer of pH 7.2.

a capacitive current was found to flow in the cathodic direction, as illustrated in Figure 9. The kinetics here (decay rate in particular) are almost the same as those of the transient photocurrents (Figure 1).

At the onset of irradiation, the interfacial pH is lowered because bR first releases a proton into the electrolyte solution, and this gives rise to a capacitive cathodic current as discussed above. This is followed by a slower process of proton uptake by bR, which recovers the interfacial pH to the initial value. Hence no current flows during continuous irradiation (for ca. 250 ms in the present experiments) where the same amount of proton is released and taken up in the bR photocycle. At the termination of irradiation, the slower process (proton uptake) entails transiently, giving rise to an anodic capacitive current. This view is corroborated by the reported photocurrent polarity reversal at lower pHs, i.e., generation of an anodic photocurrent at the onset of irradiation and a cathodic photocurrent by turning off the light,[15,16] and by invoking the reversal of the proton release/uptake sequence in the bR photocycle.

Another type of photocurrent was observed in this work, at potentials where practically no oxide is present on the gold electrode and hence we could not expect the proton dissociation equilibrium shift on the surface oxide. Though the magnitude of this photocurrent is essentially potential independent, in contrast to that at > +0.7 V, its kinetics are very similar to those found on oxide-covered electrodes. We tentatively interpret this as arising from simple charging of the electric double layer near the electrode surface due to increase/decrease in the positive charge (proton) due to photoexcitation of bR. Further work is needed to identify the exact origin of this type of photoresponse.

With experimental setups essentially different from the one used here, the flash-induced photoelectric signals from oriented purple membranes, probably due to internal charge movement associated with conformational change of bR and/or external charge movements such as proton pumping, have been detected.[27−42] The signal has at least three components with duration times lasting from picoseconds to milliseconds. The first component (B1), with a rise time shorter than 100 ps,[30,31] is thought to originate in the charge movement induced by all-trans to 13-cis isomerization of retinal.[32−34] The second component (B2), with a lifetime of 40−100 μs, is correlated with the L−M transition,[32,35−39] or partially to a proton movement from the Schiff base to Asp-85. Misra envisaged a contribution of proton release to the B2 component[40] in addition to the proton movement inside bR, as had been suggested before.[41,42] A much slower component (B3) has been observed in the millisecond regime.[15,16,29,36,38] Though the origin of this component has not been fully understood, Wang et al.[15,16] proposed that this component might correspond to the transient photocurrent under continuous excitation, namely, to the proton

release/uptake by bR. This interpretation may hold also for the photocurrents observed in the present work, since the circuit time constant (ca. 3 ms) of the potentiostatic system does not permit detection of sub-millisecond events at all.

In two-electrode systems capable of detecting rapid signals, a high degree of orientation of bR molecules is required for the observation of photoelectric responses arising from the charge polarization and protein relaxation of bR. In the present experiments, however, the orientation of bR molecules was not controlled on the surface, but the photocurrent was highly rectified. The polarity of the photocurrent would not depend on the membrane orientation, as long as the photoresponse arises, as discussed above, from the interfacial pH change due to proton release/uptake by the bR molecules. Indeed, in experiments where the photoresponse behaviors were compared between a membrane with the cytoplasmic side facing the electrode and another membrane with the extracellular side facing the electrode, the photocurrent polarity was common, and its magnitude alone depended on the membrane orientation.[13]

The transient photocurrent from bR at an electrode−electrolyte interface as employed here, revealing the activities of the proton release and uptake sites,[43] is different from the rapid photoelectric signal from oriented purple membranes by flash excitation, originating in the charge displacement within the bR molecules. These two photoelectric responses hence deliver different pieces of information about the proton-transfer processes in bR.

Acknowledgment. This work was supported in part by a Grant-in-Aid for Scientific Research on Priority Areas (Grant 09237218) from the Ministry of Education, Science and Culture of Japan.

References and Notes

(1) Oesterhelt, D.; Stoeckenius, W. *Nature New Biol.* **1971**, *233*, 149−152.
(2) Oesterhelt, D.; Stoeckenius, W. *Proc. Natl. Acad. Sci. U.S.A.* **1973**, *70*, 2853−2857.
(3) Mathies, R. A.; Lin, S. W.; Ames, J. B.; Pollard, W. T. *Annu. Rev. Biophys. Biophys. Chem.* **1991**, *20*, 491−518.
(4) Rothschild, K. J. *J. Bioenerg. Biomembr.* **1992**, *24*, 147−167.
(5) Lanyi, J. K. *Biochim. Biophys. Acta* **1993**, *1183*, 241−261.
(6) Khorana, H. G. *Proc. Natl. Acad. Sci. U.S.A.* **1993**, *90*, 1166−1171.
(7) Richter H.-T.; Brown, L. S.; Needleman, R.; Lanyi, J. K. *Biochemistry* **1996**, *35*, 4054−4062.
(8) Balashov, S. P.; Govindjee, R.; Imasheva, E. S.; Misra, S.; Ebrey, T. G. Feng, Y.; Crouch, R. K.; Menick, D. R. *Biochemistry*, **1995**, *34*, 8820−8834.
(9) Balashov, S. P.; Imasheva, E. S.; Govindjee, R.; Ebrey, T. G. *Biophys. J.* **1996**, *70*, 473−481.
(10) Miyasaka, T.; Koyama, K. *Chem. Lett.* **1991**, 1645−1648.
(11) Miyasaka, T.; Koyama, K. *Thin Solid Films* **1992**, *210/211*, 146−149.
(12) Miyasaka, T.; Koyama, K.; Itoh I. *Science* **1992**, *255*, 342−344.
(13) Koyama, K.; Yamaguchi, N.; Miyasaka T. *Science* **1994**, *265*, 762−765.
(14) Robertson, B.; Lukashev, E. P. *Biophys. J.* **1995**, *68*, 1507−1517.
(15) Wang, J.-P.; Yoo, S.-K.; Song, L.; El-Sayed, M. A. *J. Phys. Chem. B* **1997**, *101*, 3420−3423.
(16) Wang, J.-P.; Song, L.; Yoo, S.-K.; El-Sayed, M. A. *J. Phys. Chem. B* **1997**, *101*, 10599−10604.
(17) Laitinen, H. A.; Hseu, T. M. *Anal. Chem.* **1979**, *51*, 1550−1552.
(18) Fog, A.; Buck, R. P. *Sensors Actuators* **1984**, *5*, 137−146.
(19) Watanabe, T.; Gerischer, H. *J. Electroanal. Chem.* **1981**, *117*, 185−200.
(20) Oesterhelt, D.; Stoeckenius, W. *Methods Enzymol.* **1974**, *31*, 667−678.
(21) Miyasaka, T.; Watanabe, T.; Fujishima, A.; Honda, K. *J. Am. Chem. Soc.* **1978**, *100*, 6657−6664.
(22) According to the custom in electrochemistry, the cathodic and anodic currents are given here in the downward and upward directions, respectively, in a manner opposite to the one taken in previous works.[10−16.]
(23) Jones, P. G.; Rumpel, H.; Schwarzmann, E.; Sheldrick, G. M.; Paulus, H. *Acta Crystallogr.* **1979**, *B35*, 1435−1437.
(24) Schultze, J. W. *Electrochim. Acta* **1972**, *17*, 451−461.
(25) Dickinson, T.; Povey, A. F.; Sherwood, P. M. A. *J. Chem. Soc., Faraday Trans. 2* **1975**, *71*, 298−311.
(26) Besenhard, J. O.; Parsons, R.; Reeves, R. M. *J. Electrochem. Soc.* **1979**, *96*, 57−72.
(27) Trissl, H.-W. *Photochem. Photobiol.* **1990**, *51*, 793−818.
(28) Hong, F. T.; Montal, M. *Biophys. J.* **1979**, *25*, 465−472.
(29) Liu, S. Y.; Ebrey, T. G. *Biophys. J.* **1988**, *54*, 321−329.
(30) Groma, G. I.; Szabó, G.; Váró, G. *Nature* **1984**, *308*, 557−558.
(31) Trissl, H-W. *Biochim. Biophys. Acta* **1985**, *806*, 124−135.
(32) Keszthelyi, L.; Ormos, P. *Biophys. Chem.* **1983**, *18*, 397−405.
(33) Trissl, H.-W.; Gärtner, W. *Bichemistry* **1987**, *26*, 751−757.
(34) Groma, G. I.; Ráksi, F.; Szabó, G.; Váró, G. *Biophys. J.* **1988**, *54*, 77−80.
(35) Drachev, L. A.; Kaulen, A. D.; Skulachev, V. P. *FEBS Lett.* **1978**, *87*, 161−167.
(36) Keszthelyi, L.; Ormos, P. *FEBS Lett.* **1980**, *109*, 189−193.
(37) Fahr, A.; Läuger, P.; Bamberg, E. *J. Membr. Biol.* **1981**, *60*, 51−62.
(38) Ormos, P.; Hristova, S.; Keszthelyi, L. *Biochim. Biophys. Acta* **1985**, *809*, 181−186.
(39) Liu, S. Y. *Biophys. J.* **1990**, *57*, 943−950.
(40) Misra, S. *Biophys. J.* **1998**, *75*, 382−388.
(41) Liu, S. Y.; Govindjee, R.; Ebrey, T. G. *Biophys. J.* **1990**, *57*, 951−963.
(42) Liu, S. Y.; Kono, M.; Ebrey, T. G. *Biophys. J.* **1991**, *60*, 204−216.
(43) Koyama, K.; Miyasaka T.; Needleman, R.; Lanyi, J. K. *Photochem. Photobiol.* **1998**, *68*, 400−406.